PHYSICAL REVIEW B **80**, 161303(R) (2009)

Polarization phenomena in resonantly pumped disordered semiconductor microcavities

T. C. H. Liew[1] and I. A. Shelykh[2]
[1]*Centre for Quantum Technologies, National University of Singapore, Singapore 117543, Singapore*
[2]*Science Institute, University of Iceland, Dunhagi 3, IS-107 Reykjavik, Iceland*
(Received 28 August 2009; published 14 October 2009)

We analyze the spatial distribution of the intensity of photoluminescence and its polarization in resonantly pumped semiconductor microcavities. The strong spin anisotropy of polariton-polariton interactions leads to the spontaneous formation of domains with strong circular polarization in real space under a uniformly polarized elliptical pump. These domains can serve as an experimental map of the disorder profile present in the system.

DOI: 10.1103/PhysRevB.80.161303 PACS number(s): 71.36.+c, 42.65.Pc, 42.55.Sa

I. INTRODUCTION

Nonlinear optics is a rapidly developing branch of modern physics. The nonlinearity of an optical medium can lead to a variety of phenomena, including self-induced transparency, vortex formation, self-focusing, and soliton propagation. Among the most intriguing nonlinear optical effects lie bistability and multistability, resulting in a dependence of the intensity and polarization of the output of an optical system on the input pumping history.[1,2] These phenomena have been studied for more than 30 years in systems such as anisotropic crystals,[3] magnetic cavities,[4] and vertical cavity surface emitting lasers.[5] However, in the systems investigated previously, extremely high excitation powers[6] (~ 10 MW/cm^2) are required for the observation of multistable effects linked to optical nonlinearities.

Recently, it was pointed out that planar semiconductor microcavities[7] represent a unique laboratory for the study of nonlinear optical phenomena under relatively weak pump intensities (e.g., 650 W/cm^2 in Ref. 8). A semiconductor microcavity is a photonic structure designed to enhance the light-matter interaction; cavity photons are confined between two mirrors and resonantly interact with the excitonic transition of a two-dimensional (2D) semiconductor quantum well. In the strong coupling regime the normal modes of the system are cavity polaritons.[7] Being combinations of the cavity photon and 2D exciton, they have extremely small effective mass ($\sim 10^{-4}$–10^{-5} of the free electron mass, m_e) while also efficiently interacting with each other. Due to a long decoherence time[9] and the fact that in the low density limit they behave as weakly interacting bosons[10–12] the dynamics of polaritons in real space can be described by the Gross-Pitaevskii equation,[13,14] equivalent to the nonlinear Schrödinger equation of classical nonlinear optics. Polariton-polariton interactions lead to various nonlinear effects including the suppression of Rayleigh scattering,[13] parametric scattering,[15–17] bistability,[18–20] and pattern formation in real space.[21,22]

An important peculiarity of a polariton system is the spin structure of a polariton state; being formed usually by heavy-hole excitons, polaritons have two allowed spin projections on the structure growth axis (± 1), corresponding to the right and left circular polarizations of counterpart photons. In the absence of an external magnetic field the "spin-up" and "spin-down" states of noninteracting polaritons or their linearly polarized superpositions are degenerate. The situation changes if polariton-polariton scattering is accounted for: the interaction of polaritons in triplet configuration (parallel spin projections on the structure growth axis) is much stronger than that of polaritons in singlet configuration (antiparallel spin projections).[23,24] This leads to a mixing of linearly polarized polariton states which manifests itself in remarkable nonlinear effects in polariton spin relaxation, such as self-induced Larmor precession and inversion of linear polarization upon scattering.[25]

Another timely topic in the field of microcavity physics is the influence of disorder on the properties of cavity polaritons. Almost all existing experimental data clearly show strong localization of polariton condensates due to the structural photonic imperfections[10,26] and signatures of superfluidity have been reported only very recently.[27,28] The theoretical description of polariton dynamics in a nonresonantly pumped disordered cavity in terms of a transition from a glassy to a superfluid phase was recently given.[29] However, the interplay between spin anisotropy of polariton-polariton interactions and disorder was completely neglected.

In the present Rapid Communication we analyze the polarization sensitive behavior of a resonantly pumped microcavity with a long-range (photonic) disorder, which was shown to affect crucially the properties of cavity polaritons.[30] We are particularly interested in the behavior of polarized domain walls, which requires the use of the nonlinear Gross-Pitaevskii equation[13] accounting for the two polarization states[31] so as to allow polarization multistability of resonantly driven polariton modes. The interplay between polarization multistability and long-range photonic disorder causes polarization resolved spatial images to directly resemble the structure of disorder allowing its experimental mapping. Given the importance of the disorder profile in many microcavity experiments, for example, in the optical spin Hall effect[32] or experiments searching for superfluidity (involving scattering with a defect[13,28]), we believe that the polarization mapping of disorder will become an important experimental tool. We calculate the distribution of the photoluminescence intensity and its polarization for the cases of optical excitation at normal incidence (directly generating polaritons with $k=0$) as well as magic angle excitation[15–17] [under which pairs of pumped polaritons scatter into signal ($k \approx 0$) and idler states].

Although imaging of optical disorder has been experimentally demonstrated by spatially resolving the emission of a polariton condensate,[10,26] we expect the technique that we propose can offer higher resolution. We exploit sharp domain walls and are unaffected by the complicated energy relaxation dynamics of polaritons, which involves traveling polaritons as intermediate states. Furthermore we are relying on a classical optical effect and we expect that some of the challenging conditions required for polariton condensation can be relaxed, for example, we expect that optical bistability is much more resilient to phonon scattering. Finally, since we excite polaritons at energies not too far from resonance, much lower excitation powers can be used.

II. PUMPING AT NORMAL INCIDENCE

First, we consider the case of optical excitation at normal incidence. If one neglects the upper polariton branch (the pump energy lies below the upper branch energy, so upper branch polaritons are not excited), the polariton field is described by a pair of wave functions ψ_σ, which satisfy the driven spinor Gross-Pitaevskii equation,[31]

$$i\hbar\frac{\partial\psi_\sigma}{\partial t} = (\hat{E}_{LP} + U + \alpha_1|\psi_\sigma|^2 + \alpha_2|\psi_{-\sigma}|^2)\psi_\sigma + p_\sigma, \quad (1)$$

where $\sigma = \pm 1$ labels right and left circular polarizations. $\hat{E}_{LP}$ is the kinetic energy operator of lower branch polaritons, which can be written in reciprocal space as

$$E_{LP}(\vec{k}) = \frac{E_C(\vec{k}) - E_X(\vec{k})}{2} - \frac{1}{2}\sqrt{[E_X(\vec{k}) - E_C(\vec{k})]^2 + \Omega^2}, \quad (2)$$

where the exciton energy levels, $E_X(\vec{k})$, and photon energy levels, $E_C(\vec{k})$, are characterized by effective masses, m_X and m_C (here we assume zero detuning between the photon and exciton modes at $\vec{k}=0$),

$$E_{C,X}(\vec{k}) = \frac{\hbar^2|\vec{k}|^2}{2m_{C,X}} - \frac{i\hbar}{\tau_{C,X}}. \quad (3)$$

The phenomenological lifetimes, τ_X and τ_C, account for exciton recombination and photon escape. Ω is the Rabi splitting (twice the exciton-photon coupling energy). U is a random spatially varying disorder potential [see Fig. 1(b)] characterized by a correlation length, l, and root mean squared amplitude U_{rms}. The potential was generated using the same method as in Ref. 33. We assume the disorder to be spin independent. $\alpha_{1(2)}$ are matrix elements of the polariton-polariton interaction in the triplet (singlet) configuration. Polariton-polariton interactions are strongly anisotropic and normally $\alpha_1 > 0$, $\alpha_2 < 0$, $|\alpha_2| \ll \alpha_1$.[23] The polarized optical excitation is defined by $p_\sigma = f_\sigma e^{-iE_p t/\hbar}$, where f_σ can vary both in space and time. E_p is the pump energy. We neglect any $\vec{k}$-dependent susceptibility of the pump, which would only be important if we used wide distributions in $\vec{k}$ space. Nonuniform absorption in space is automatically accounted for by the disorder potential, U.

Before presenting our results, let us summarize qualitatively the effects of polarization multistability by considering the state of polaritons at a single point in space, neglecting coupling to neighboring states (i.e., in the limit of infinite polariton mass, also known as the Thomas-Fermi approximation). Imagine the pump is oriented at normal incidence, such that polaritons are excited with zero in-plane wave vector. In the stationary regime[31] Eq. (1) yields a cubic dependence of the polariton intensity, $n_\sigma = |\psi_\sigma|^2$, on the pump intensity, $P_\sigma = |p_\sigma|^2$,

$$\left[(\Delta + \alpha_1 n_\sigma + \alpha_2 n_{-\sigma})^2 + \frac{\hbar^2}{4\tau^2}\right] n_\sigma = P_\sigma, \quad (4)$$

where $\Delta = E_0 - E_p$ is the detuning between the bottom of the lower polariton branch, E_0, and the optical pump. τ is the effective polariton lifetime. Supposing that $\alpha_2 = 0$, the dependence of the internal polariton intensities on the pump intensity is an S-shaped curve (identical for the two polarized components, $\sigma = \pm 1$), as shown in Fig. 1(a).

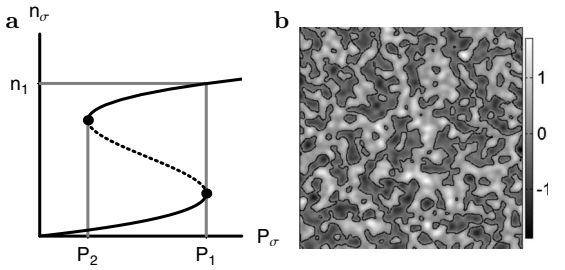

FIG. 1. (a) The spinor polariton population, n_σ, as a function of pumping intensity, P_σ, for a single polariton state. With increasing intensity, the population, n_σ, jumps when $P_\sigma = P_1$ to the upper branch of the bistability curve. (b) Amplitude of a randomly generated disorder potential, U, characterized by $U_{\text{rms}} = 0.5$ meV and $l = 5$ μm [these parameters are roughly inferred from experiments on polariton condensation (Ref. 26)]. The black lines show contours along which $U = 0$.

It is useful to define the circular polarization degree of a polariton state as $\rho_c = (n_+ - n_-)/(n_+ + n_-)$. If, when the external pump is switched on, $P_+, P_- \leq P_1$ then the solutions for the internal fields, n_+ and n_-, both lie on the lower branch of the S-shaped curve. In this case $\rho_c \approx \rho_c^{pump}$, where $\rho_c^{pump} = (P_+ - P_-)/(P_+ + P_-)$ is the circular polarization degree of the pump. On the other hand, if $P_- \leq P_1 \leq P_+$ then the solution for the σ^+ polarized internal field switches to the upper branch of the S-shaped curve while the solution for the σ^- polarized internal field remains on the lower branch. Consequently, the internal field is strongly circularly polarized; $\rho_c \approx 1$ even if $\rho_c^{pump} \ll 1$. Finally, if $P_+, P_- > P_1$ the solutions for both polarizations lie on the upper branch and the situation $\rho_c \approx \rho_c^{pump}$ is recovered. If one then starts to decrease the pump intensity then the reverse switching between upper and lower branches occurs at a different point, P_2, leading to the appearance of hysteresis not only in the total intensity of the internal polariton field but also in its circular polarization degree.[31] One can imagine an optical memory element based on this hysteresis.[22]

Now let us consider the influence of disorder. For some qualitative understanding let us again consider the case of polaritons with an infinite effective mass. In this case their

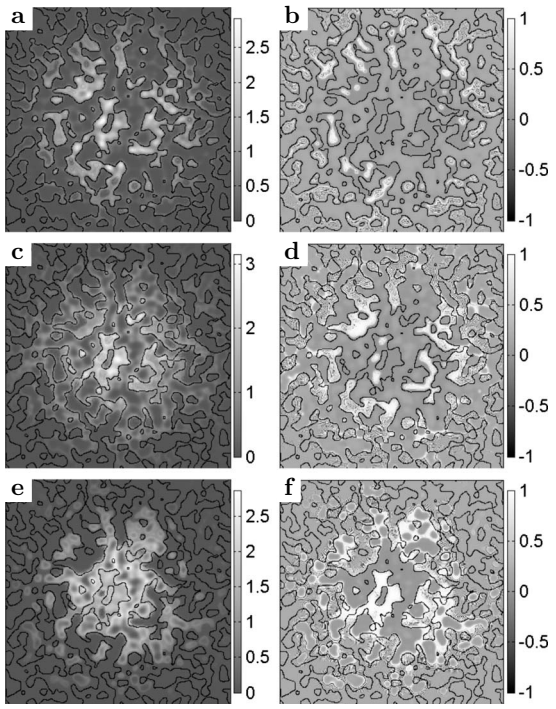

FIG. 2. The polariton field in a 0.4×0.4 mm^2 area in real space under Gaussian cw excitation at normal incidence with $\rho_c^{pump}=0.2$. Left-hand plots show the total intensity (arbitrary units) of the polariton field, $n_+ + n_-$; right-hand plots show the circular polarization degree, ρ_c. The different rows correspond to different (spatially averaged) detuning: (a) and (b) $\langle\Delta\rangle=0$ meV; (c) and (d) $\langle\Delta\rangle=-0.5$ meV; and (e) and (f) $\langle\Delta\rangle=-1$ meV. The disorder potential was the same as the one plotted in Fig. 1(b) and black lines again represent contours along which $U=0$. Parameters: $m_C=10^{-4}m_e$, $m_X=0.22m_e$, $\alpha_2/\alpha_1=-0.1$, $\tau=3$ ps, and $U_{\rm rms}=0.5$ meV. The Gaussian pump had a full width at half maximum of 100 μm.

in-plane propagation is blocked. Due to the presence of the disorder potential the detuning, $\Delta=\Delta(\mathbf{r})$, becomes position dependent. Consequently, the shape of the S-shaped curve [Fig. 1(a)] is different at different points, causing the total intensity and circular polarization degree to also become spatially dependent; in some places both n_+ and n_- lie on the upper branch of the S-shaped curve, while at others they both lie on the lower branch or n_+ lies on the upper branch while n_- lies on the lower branch. The account of a finite effective mass can smear this picture a little, but a strong spatial dependence of the polariton field survives, which mimics the spatial dependence of the disorder potential.

Solving Eq. (1) numerically (with finite polariton mass) yields the results plotted in Fig. 2. The results depend on the (spatially averaged) detuning, $\langle\Delta\rangle$. The pump intensity is fixed. When the average detuning is zero [Figs. 2(a) and 2(b)] the average value of P_1 is exceeded by the pump intensity in both polarizations at most points, such that $\rho_c\approx0$. In fact many points do not exhibit bistability at all since one must have $\Delta<-\sqrt{3}\hbar/\tau$ for a bistable curve.[18–20] Only a few points far from the center of the pump spot, where the pump intensity is weak, show significant polarization degree. As $\langle\Delta\rangle$ is decreased [Figs. 2(e) and 2(f)], by increasing the pump

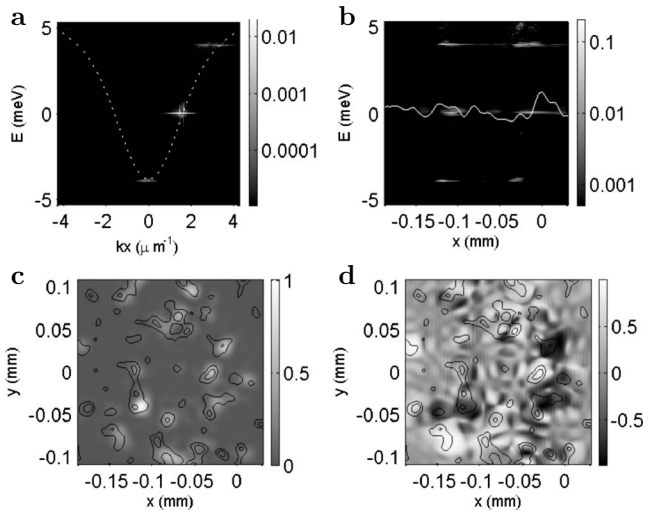

FIG. 3. Plots of the polariton field under a Gaussian cw excitation at magic angle with $\rho_c^{pump}=0.2$. (a) Energy-momentum dispersion diagram of the polariton intensity. The dotted white curve shows the dependence of the polariton eigenergy on the wave vector (spatially averaged). (b) The energy distribution of polaritons in space. The white curve shows the distribution of the polariton potential. (c) The distribution of the signal intensity in real space. (d) The circular polarization degree of the signal in real space. In (c) and (d) the black curves show contours in the disorder potential at −0.5 and −1 meV. Parameters were the same as in Fig. 2 but $\vec{k}_p=1617$ mm^{-1}, $\Omega=10$ meV, $E_p=E_{LP}(\vec{k}_p)$, $m_C=10^{-5}m_e$, $\tau_C=1.3$ ps, and $\tau_X=100$ ps.

energy, the effect of the disorder on the polarization becomes more significant. The locus of points along which ρ_c suddenly jumps tends to follow the contours in the disorder potential (shown by black lines). In this sense one can imagine using a polarization resolved image of the microcavity photoluminescence to map the disorder profile.

III. PARAMETRIC OSCILLATOR CONFIGURATION

Currently in the field of microcavities, many experiments focus on excitation at magic angle,[15–17] where energy and momentum conservation laws allow the scattering of pairs of pumped polaritons with $k=k_p$ into signal states with $k=0$ and idler states with $k_i=2k_p$. Since this is a popular excitation scheme, an obvious question is whether the disorder potential can be mapped by mapping the signal distribution of an optical parametric oscillator (OPO).

Theoretically, an optical pump at oblique angle modulates the spatial dependence of p_σ by a factor e^{ik_px}, where k_p is the in-plane wave vector of injected polaritons. Making this change and again solving Eq. (1) numerically yields the results in Fig. 3. In Fig. 3(a) the spectral (energy) distribution of polaritons is shown in reciprocal space (along an axis parallel to $\vec{k}_p$), clearly demonstrating the parametric scattering of polaritons to the signal ($k=0$) state. Figure 3(b) shows the spectral distribution along a slice in real space (along an axis parallel to $\vec{k}_p$). The disorder potential is also shown by the white curve. The disorder potential changes the polariton eigenenergy at different points, which alters the stability of

pump, signal, and idler modes.[20,34] The signal intensity does tend to follow contours in the disorder potential as shown in Fig. 3(c). However, the behavior of ρ_c in space does not.

An understanding of parametric scattering in the OPO can be derived from Refs. 20 and 34 where a three mode coupled system was considered neglecting the polarization degree of freedom. Given that we pump elliptically we expect the intricate effects reported in their work to have a complicated polarization sensitivity—a treatment of which goes far beyond the scope of our work. Furthermore, we are aware of effects such as self-induced Larmor precession, polarization inversion upon parametric scattering, and spreading effects of domain walls.[35] An understanding of how these effects interplay is an open question, although all these effects are accounted for in our numerical model. Our conclusion is that polarization mapping of a disorder potential is not feasible under the parametric oscillator excitation scheme, although excitation near normal incidence remains promising.

IV. CONCLUSIONS

We considered the effect of the spatially varying disorder in semiconductor microcavities upon the intensity and polarization of resonantly pumped exciton polaritons. It was shown that, under excitation at both normal incidence and magic angle, domains with strong circular polarization degree develop. We believe that the considered effect provides a simple but previously unused method (using excitation near normal incidence) for imaging the disorder potential in microcavities; one need only take a polarization resolved image of the photoluminescence rather than measure dispersion curves at every point across the sample. Furthermore, by relying on domain walls the characterization can be particularly accurate. Indeed the disorder present in microcavities has a significant influence on all imaginable experiments and for some it is even an essential ingredient. It is obvious that experimentally measured maps of the disorder potential would allow a better understanding of this influence in many cases.

ACKNOWLEDGMENT

We thank A. V. Kavokin and G. Malpuech for useful discussions.

[1] M. I. Dykman, Sov. Phys. JETP **64**, 927 (1986).
[2] M. I. Dykman and A. L. Velikovich, Opt. Commun. **70**, 151 (1989).
[3] J. Yumoto and K. Otsuka, Phys. Rev. A **34**, 4445 (1986).
[4] F. Jonsson and C. Flytzanis, Phys. Rev. Lett. **82**, 1426 (1999).
[5] M. Sciamanna and K. Panajotov, Phys. Rev. A **73**, 023811 (2006).
[6] N. I. Zheludev, Sov. Phys. Usp. **32**, 357 (1989).
[7] A. V. Kavokin, J. J. Baumberg, G. Malpuech, and F. P. Laussy, *Microcavities* (Oxford University Press, New York, 2007).
[8] V. D. Kulakovskii *et al.*, Phys. Usp. **43**, 853 (2000).
[9] W. Langbein, I. Shelykh, D. Solnyshkov, G. Malpuech, Y. Rubo, and A. Kavokin, Phys. Rev. B **75**, 075323 (2007).
[10] J. Kasprzak *et al.*, Nature (London) **443**, 409 (2006).
[11] R. Balili *et al.*, Science **316**, 1007 (2007).
[12] C. W. Lai *et al.*, Nature (London) **450**, 529 (2007).
[13] I. Carusotto and C. Ciuti, Phys. Rev. Lett. **93**, 166401 (2004).
[14] I. A. Shelykh, Y. G. Rubo, G. Malpuech, D. D. Solnyshkov, and A. Kavokin, Phys. Rev. Lett. **97**, 066402 (2006).
[15] P. G. Savvidis, J. J. Baumberg, R. M. Stevenson, M. S. Skolnick, D. M. Whittaker, and J. S. Roberts, Phys. Rev. Lett. **84**, 1547 (2000).
[16] A. I. Tartakovskii, D. N. Krizhanovskii, and V. D. Kulakovskii, Phys. Rev. B **62**, R13298 (2000).
[17] M. Saba *et al.*, Nature (London) **414**, 731 (2001).
[18] A. Baas, J. P. Karr, M. Romanelli, A. Bramati, and E. Giacobino, Phys. Rev. B **70**, 161307(R) (2004).
[19] N. A. Gippius *et al.*, Europhys. Lett. **67**, 997 (2004).
[20] D. M. Whittaker, Phys. Rev. B **71**, 115301 (2005).
[21] A. V. Yulin, O. A. Egorov, F. Lederer, and D. V. Skryabin, Phys. Rev. A **78**, 061801(R) (2008).
[22] I. A. Shelykh, T. C. H. Liew, and A. V. Kavokin, Phys. Rev. Lett. **100**, 116401 (2008).
[23] M. Combescot and O. Betbeder-Matibet, Phys. Rev. B **74**, 125316 (2006).
[24] C. Ciuti, V. Savona, C. Piermarocchi, A. Quattropani, and P. Schwendimann, Phys. Rev. B **58**, 7926 (1998).
[25] D. N. Krizhanovskii, D. Sanvitto, I. A. Shelykh, M. M. Glazov, G. Malpuech, D. D. Solnyshkov, A. Kavokin, S. Ceccarelli, M. S. Skolnick, and J. S. Roberts, Phys. Rev. B **73**, 073303 (2006).
[26] J. Kasprzak, R. Andre, L. S. Dang, I. A. Shelykh, A. V. Kavokin, Y. G. Rubo, K. V. Kavokin, and G. Malpuech, Phys. Rev. B **75**, 045326 (2007).
[27] S. Utsunomiya *et al.*, Nat. Phys. **4**, 700 (2008).
[28] A. Amo *et al.*, Nature (London) **457**, 291 (2009).
[29] G. Malpuech, D. D. Solnyshkov, H. Ouerdane, M. M. Glazov, and I. Shelykh, Phys. Rev. Lett. **98**, 206402 (2007).
[30] V. Savona, J. Phys.: Condens. Matter **19**, 295208 (2007).
[31] N. A. Gippius, I. A. Shelykh, D. D. Solnyshkov, S. S. Gavrilov, Y. G. Rubo, A. V. Kavokin, S. G. Tikhodeev, and G. Malpuech, Phys. Rev. Lett. **98**, 236401 (2007).
[32] C. Leyder *et al.*, Nat. Phys. **3**, 628 (2007).
[33] V. Savona and W. Langbein, Phys. Rev. B **74**, 075311 (2006).
[34] M. Wouters and I. Carusotto, Phys. Rev. B **75**, 075332 (2007).
[35] T. C. H. Liew, A. V. Kavokin, and I. A. Shelykh, Phys. Rev. Lett. **101**, 016402 (2008).